Weak Ergodicity Breaking and Aging of Chaotic Transport in Hamiltonian Systems

Tony Albers* and Günter Radons†
Institute of Physics, Technische Universität Chemnitz, 09107 Chemnitz, Germany
(Received 11 July 2014; published 31 October 2014)

Momentum diffusion is a widespread phenomenon in generic Hamiltonian systems. We show for the prototypical standard map that this implies weak ergodicity breaking for the superdiffusive transport in coordinate direction with an averaging-dependent quadratic and cubic increase of the mean-squared displacement (MSD), respectively. This is explained via integrated Brownian motion, for which we derive aging time dependent expressions for the ensemble-averaged MSD, the distribution of time-averaged MSDs, and the ergodicity breaking parameter. Generalizations to other systems showing momentum diffusion are pointed out.

DOI: 10.1103/PhysRevLett.113.184101 PACS numbers: 05.45.-a, 05.40.-a, 05.60.-k

Anomalous diffusion has long been recognized as an important transport mechanism occurring in physical, chemical, biological, and sociological systems [1–3]. It has been observed, e.g., for charge-carrier transport in amorphous semiconductors [4], diffusion in porous materials [5] and living cells [6], travel behavior of humans [7], and for chaotic transport in the phase space of nonintegrable Hamiltonian systems [8–10], where the latter is important for different fields such as transport of passively advected tracers in two-dimensional, incompressible flows [11] and the motion of charged particles in magnetized plasmas [12]. A mechanism that can lead to anomalous diffusion in Hamiltonian systems is the occurrence of momentum diffusion. In this case, the corresponding coordinate shows superdiffusive behavior with a mean-squared displacement (MSD) which asymptotically increases according to a power law, $\langle \Delta x^2(\tau) \rangle \sim \langle D_\alpha \rangle \tau^\alpha$, where the diffusion exponent α is larger than one, and $\langle D_\alpha \rangle$ is the generalized diffusion coefficient [13]. A fundamental aspect of anomalous diffusion, which has moved both physicists and biologists in recent years, is the question of ergodicity, i.e., the equivalence of the ensemble- and time-averaged MSD [15,16]. For subdiffusive ($\alpha < 1$) continuous time random walks [17] with a waiting time distribution which has no finite mean, weak ergodicity breaking and aging have been found [18–21], whereas fractional Brownian motion [22] and diffusion on fractal supports [23] are ergodic with respect to the squared displacements [24,25]. Weak ergodicity breaking was originally introduced in the context of spin-glasses [26] and has been experimentally observed, for instance, for blinking quantum dots [27] and for diffusion of lipid granules in yeast cells [28]. In contrast to strong ergodicity breaking, the underlying state or phase space of these systems is not divided into mutually inaccessible regions. Instead, the diverging characteristic time scale of the process can be regarded as the origin of the nonergodic behavior. Weak ergodicity breaking has also been found for a special heterogeneous diffusion process [29], which can be either sub- or superdiffusive, while for Lévy walks [30] with constant velocity, nonergodic behavior only occurs in the ballistic case ($\alpha = 2$) [31,32].

Despite this large variety of investigations, to our knowledge, weak ergodicity breaking has not been reported for Hamiltonian systems in the literature so far. This is the aim of this Letter. We will show that the transition to global stochasticity, i.e., the occurrence of momentum diffusion on global scales, entails weak ergodicity breaking and aging for the diffusive transport in coordinate direction, where the latter is well described by integrated Brownian motion. This stochastic model allows an exact analytical derivation of the quantities of interest due to its simplicity but, nevertheless, confirms the complex behavior which is found for Hamiltonian systems. Momentum diffusion is a typical phenomenon in Hamiltonian systems [33] and has also been found in branched flows [34,35], which occur in many branches of science [36,37], for scattering processes in disordered systems [38,39], and for a system of two coupled, kicked quantum rotors [40]. Furthermore, integrated Brownian motion, or equivalently the dynamics of randomly accelerated particles [41,42], plays a role, for instance, for the statistical physics of polymer chains [43] and, most importantly, is related to the Richardson-Obukhov law of passive tracer transport in turbulent flows [44,45]. The latter was also observed under certain conditions for diffusion of cold atoms in optical lattices [46] and the Brownian motion of an optically trapped particle in air [47]. In all these systems, our results, reported below, play a role and, in principle, can be observed experimentally.

In the following, we investigate one of the simplest examples for the occurrence of momentum diffusion, the standard map [48]

$$p_{t+1} = p_t + \frac{k}{2\pi} \sin(2\pi x_t), \tag{1}$$

$$x_{t+1} = x_t + p_{t+1}, \tag{2}$$

which has become a paradigmatic example because it shows all the phenomena typical for low-dimensional, nonintegrable Hamiltonian chaos and, especially, a transition to global stochasticity, where momentum diffusion sets in. We emphasize, however, that our findings are not restricted to low-dimensional systems. For the standard map, there is a critical perturbation strength, $k_c = 0.9716\ldots$, for which the last invariant Kolmogorov-Arnold-Moser (KAM) curve in phase space running from $x = -\infty$ to $x = \infty$ is destroyed [49]. Above this critical perturbation, diffusion in momentum direction occurs [50,51]. For our numerical simulations, we choose $k = 1.5$. Following MacKay [53], the corresponding diffusion coefficient is given by $\langle D_1 \rangle = 0.0012$. This value agrees very well with our numerical simulations (not shown in the figures). If the motion in momentum direction is well described by normal diffusion, the motion in coordinate direction, Eq. (2), can be regarded as the Euler discretization of integrated Brownian motion (IBM). In the following, we study this stochastic process and compare our analytical results with quantities numerically obtained from the deterministic standard map.

Integrated Brownian motion [54–56] is defined by

$$\ddot{x}(t) = \xi(t) \rightarrow x(t) = x(0) + \int_0^t W(t')dt', \tag{3}$$

where $\xi(t)$ is Gaussian white noise and $W(t)$ is the Wiener process with mean value $\langle W(t) \rangle_{\mathrm{E}} = W_0$ and covariance function $C_W(t,s) = \langle W(t)W(s) \rangle_{\mathrm{E}} - \langle W(t) \rangle_{\mathrm{E}} \langle W(s) \rangle_{\mathrm{E}} = \langle D_1 \rangle \min(t,s)$. We use the symbols $\langle \ldots \rangle_{\mathrm{E}}$ and $\langle \ldots \rangle_{\mathrm{T}}$ for ensemble and time averages, respectively. For simplicity, we set $W_0 = 0$. How a nonvanishing W_0 influences the following results in a trivial and, also, in a nontrivial way will be discussed elsewhere [57]. The covariance function of IBM is well known [56]

$$C_{\mathrm{IBM}}(t,s) = \langle D_1 \rangle \left(\frac{s^2 t}{2} - \frac{s^3}{6} \right), \qquad t > s. \tag{4}$$

From this, we can calculate the ensemble-averaged MSD, and we obtain

$$\langle \Delta x^2(\tau) \rangle_{\mathrm{E}} = \langle [x(t_a + \tau) - x(t_a)]^2 \rangle_{\mathrm{E}} = \langle D_1 \rangle \left(t_a \tau^2 + \frac{\tau^3}{3} \right), \tag{5}$$

where t_a is the so-called aging time, the elapsed time between the beginning of the process and the beginning of the measurement. Figure 1 shows a very good agreement between our theoretical result and numerically determined MSDs for the diffusion in coordinate direction in the phase space of the standard map. Obviously, the diffusion exponent depends on the aging time. For $\tau \ll t_a$ we observe $\alpha = 2$, while asymptotically, for $\tau \gg t_a$ we have $\alpha = 3$.

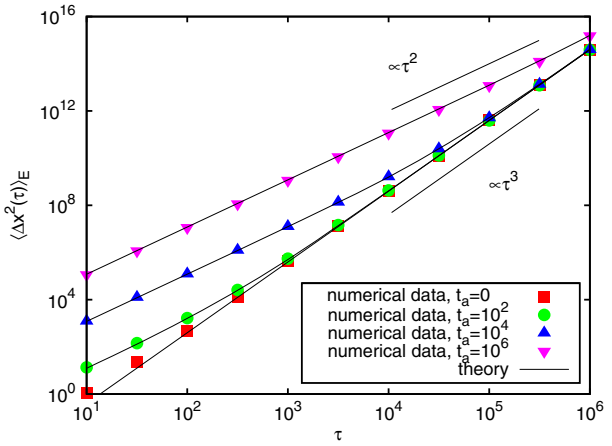

FIG. 1 (color online). Ensemble-averaged MSD for different aging times t_a numerically obtained from $N = 5 \times 10^5$ trajectories generated by the standard map for $k = 1.5$. The trajectories were started close to the hyperbolic fixed point at $(x, p) = (0, 0)$. Also shown in the figure is the theoretical result of Eq. (5), which was derived from integrated Brownian motion.

This behavior should be contrasted with the behavior of the time-averaged MSD defined as

$$\langle \Delta x^2(\tau) \rangle_{\mathrm{T}} = \frac{1}{T - \tau} \int_{t_a}^{t_a + T - \tau} [x(t + \tau) - x(t)]^2 dt. \tag{6}$$

By using Eq. (5), we can calculate the ensemble average of the time average, Eq. (6), and we get

$$\langle \langle \Delta x^2(\tau) \rangle_{\mathrm{T}} \rangle_{\mathrm{E}} = \langle D_1 \rangle \left((2t_a + T) \frac{\tau^2}{2} - \frac{\tau^3}{6} \right). \tag{7}$$

In Fig. 2, we can see four numerically determined time-averaged MSDs for the diffusion in coordinate direction. Despite the very long observation time of $T = 2 \times 10^{10}$, the time-averaged MSD remains random in the sense that the generalized diffusion coefficient varies from one trajectory to another. Therefore, ergodicity is broken. The diffusion exponent $\alpha = 2$, which is predicted by Eq. (7) for long observation times $T \gg \tau$, is the same for every trajectory. In the rest of the Letter, we will characterize the randomness of the time-averaged MSD analytically and numerically.

For this purpose, we investigate the dimensionless random variable $\hat{\xi}(\tau)$ whose probability density is given by

$$p(\xi;\tau) = \left\langle \delta\left(\xi - \frac{\langle \Delta x^2(\tau) \rangle_{\mathrm{T}}}{\langle \langle \Delta x^2(\tau) \rangle_{\mathrm{T}} \rangle_{\mathrm{E}}} \right) \right\rangle_{\mathrm{E}} \overset{T \gg \tau}{\rightarrow} p(\xi). \tag{8}$$

Because of the rescaling and the behavior of the time-averaged MSD shown in Fig. 2, this distribution does not depend on the time lag τ for $T \gg \tau$. $p(\xi)$ was recently

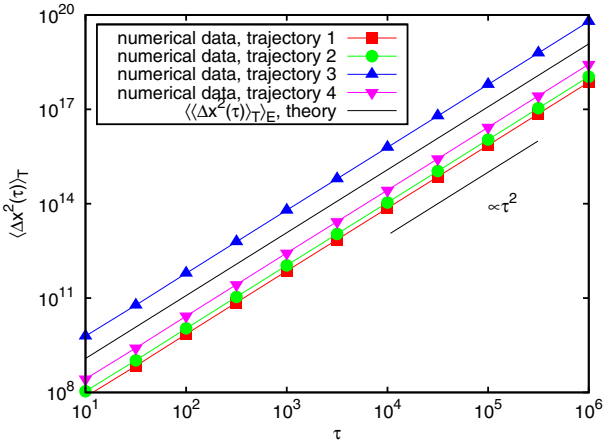

FIG. 2 (color online). Time-averaged MSD ($t_a = 0$) of four different trajectories of length $T = 2 \times 10^{10}$ numerically generated by the standard map for $k = 1.5$. Again, all trajectories were started close to the hyperbolic fixed point at $(x, p) = (0, 0)$. The theoretical curve corresponds to Eq. (7) and describes the ensemble average of time-averaged MSDs for integrated Brownian motion.

studied for subdiffusive continuous time random walks [20,21], Lévy walks [31,32], and a special heterogeneous diffusion process [29]. The mean of $\hat{\xi}(\tau)$ is equal to unity, and for an ergodic process, we have $p(\xi;\tau) = \delta(\xi - 1)$ for $T \to \infty$. As a first step towards an analytical derivation of the probability density $p(\xi)$ for integrated Brownian motion, we consider another dimensionless random variable $\xi^*(t) = C_v(t)/\langle C_v(t)\rangle_{\mathrm{E}}$, where $C_v(t) = (T-t)^{-1}\int_{t_a}^{t_a+T-t} W(t'+t)W(t')dt'$ is the autocorrelation function defined as time average over the corresponding velocity process, the Wiener process in our case. The ensemble average of this function is given by $\langle C_v(t)\rangle_{\mathrm{E}} = \langle D_1\rangle(2t_a + T - t)/2$. Again, due to the rescaling, the random variable $\xi^*(t)$ does not depend on the time lag t for $T \gg t$. In this case, we can replace $\xi^*(t)$ by $\xi^*(t = 0)$. This is confirmed by our numerical simulations, which are not shown here. By using the Green-Kubo formula [58] $\langle \Delta x^2(\tau)\rangle_{\mathrm{T}} = 2\int_0^\tau (\tau - t)C_v(t)\mathrm{d}t$, we can prove that the random variables $\hat{\xi}(\tau)$ and $\xi^*(t=0)$ are equal in distribution for $T \gg \tau$. Therefore, in the following, we treat $\xi^*(t=0) = 2[\langle D_1\rangle(2t_a + T)T]^{-1}\int_{t_a}^{t_a+T} W^2(t)\mathrm{d}t$. In order to find an analytical expression for the Laplace transform $\tilde{p}(s) = \langle \exp\{-2s[\langle D_1\rangle(2t_a + T)T]^{-1}\int_{t_a}^{t_a+T} W^2(t)dt\}\rangle_{\mathrm{E}}$ of the probability density of the random variable $\xi^*(t=0)$, we use the Feynman-Kac formalism [59]. For this purpose, we write the Laplace transform in terms of a path integral,

$$\tilde{p}(s) = \int_{-\infty}^{\infty}\int_{-\infty}^{\infty}\left\{\int_{W(t_a)=x_0}^{W(t_a+T)=x} \exp\left(-\frac{1}{2\langle D_1\rangle}\int_{t_a}^{t_a+T}\dot{W}^2(t)dt - \frac{2s}{\langle D_1\rangle(2t_a+T)T}\int_{t_a}^{t_a+T} W^2(t)dt\right)\mathcal{D}[W(t)]\right\} \times \frac{1}{\sqrt{2\pi\langle D_1\rangle t_a}}\exp\left(-\frac{x_0^2}{2\langle D_1\rangle t_a}\right)dx_0dx, \tag{9}$$

where we integrate over all Wiener trajectories which are at position x_0 at time t_a and at position x at time $t_a + T$. In Eq. (9), we multiply the path integral with the probability to actually be at position x_0 at time t_a and then integrate over x_0 and x. The path integral can be solved by comparing it with the known propagator of the quantum harmonic oscillator. Then, performing the two integrations in Eq. (9), we obtain

$$\tilde{p}(s) = \left[\sqrt{\frac{4s\lambda^2}{1+2\lambda}}\sinh\left(\sqrt{\frac{4s}{1+2\lambda}}\right) + \cosh\left(\sqrt{\frac{4s}{1+2\lambda}}\right)\right]^{-(1/2)}. \tag{10}$$

This is our main result, which only depends on the ratio $\lambda = t_a/T$. In Fig. 3, we compare it with numerically determined distributions $p(\xi)$ for the diffusion in coordinate direction in the phase space of the standard map. We can see a very good agreement. For the numerical Laplace inversion of Eq. (10), we used the method described in [60]. We would like to mention that the probability distribution

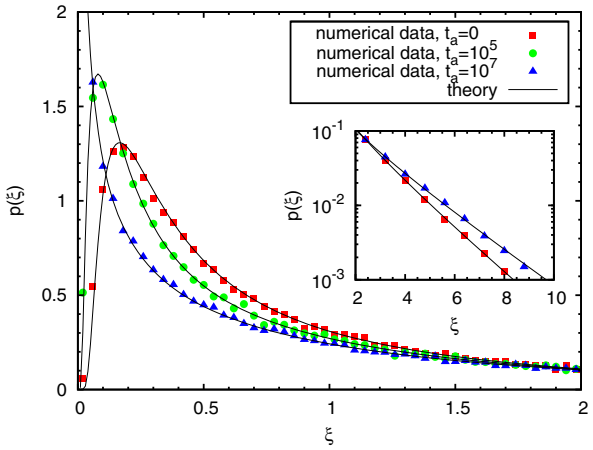

FIG. 3 (color online). Scatter distribution of rescaled time-averaged MSDs ($\tau = 100$) for three different aging times t_a numerically determined from $N = 10^5$ trajectories of length $T = 10^5$ generated by the standard map for $k = 1.5$. The numerical data agree very well with the theoretical curves, which were obtained from a numerical Laplace inversion of Eq. (10).

of the random variable $\xi^*(t=0)$ can also be obtained by the Cameron-Martin theorem, which is known in the mathematical literature [61], or by using the formula on page 124 in [62]. For $t_a = 0$, Eq. (10) simplifies to

$$\tilde{p}(s) \overset{t_a=0}{=} [\cosh(\sqrt{4s})]^{-(1/2)}. \quad (11)$$

This formula is known as the Cameron-Martin generating function for the random variable $\int_0^1 W^2(t)dt$. The corresponding asymptotic behavior in the original space is given by $(2\pi\xi^3)^{-(1/2)}\exp[-1/(4\xi)]$ for $\xi \to 0$ and $(2\sqrt{\xi})^{-1}\exp[-(\pi^2/16)\xi]$ for $\xi \to \infty$.

Figure 3 shows the dependence of the distribution $p(\xi)$ on the aging time t_a. For every finite t_a, $p(\xi = 0) = 0$, but with increasing aging time, the maximum of the distribution $p(\xi)$ becomes narrower and larger and gets closer to $\xi = 0$ in the sense that $p(\xi)$ approaches for $t_a \to \infty$ the limit distribution $(2\pi\xi)^{-(1/2)}\exp(-\frac{1}{2}\xi)$.

Finally, we consider the ergodicity breaking parameter EB [20], which is defined as the variance of the random variable $\hat{\xi}(\tau)$, and which is equal to zero for an ergodic process in the limit $T \to \infty$. It can be calculated for integrated Brownian motion for $T \gg \tau$ from Eq. (10)

$$\mathrm{EB} = \langle\hat{\xi}(\tau)^2\rangle_{\mathrm{E}} - \langle\hat{\xi}(\tau)\rangle_{\mathrm{E}}^2 = \frac{4}{3}\left[1 + \frac{2}{(2+1/\lambda)^2}\right]. \quad (12)$$

The ergodicity breaking parameter only depends on the ratio $\lambda = t_a/T$ and grows from 4/3 to 2 with increasing λ. Figure 4 shows a comparison between the numerically determined ergodicity breaking parameter for the diffusion in coordinate direction in the phase space of the standard map and the result from Eq. (12). Again, we can observe a very good agreement.

We want to summarize and discuss our findings. We have seen that the motion in coordinate direction in the phase space of the standard map is well described by integrated Brownian motion if the diffusion process in momentum direction is normal. Integrated Brownian motion exhibits aging and weak ergodicity breaking. The ensemble-averaged MSD increases asymptotically as τ^3, but depends on the aging time t_a insofar as it increases only quadratically in the preasymptotic regime $\tau \ll t_a$. In contrast, the time-averaged MSD increases always as τ^2, and in addition, it is random in the sense that each trajectory gives a different generalized diffusion coefficient. The randomness of the time-averaged MSD is described by a broad scatter distribution and a nonvanishing ergodicity breaking parameter, which increases with growing aging time. We know from other diffusion processes, such as subdiffusive continuous time random walks or ballistic Lévy walks, that the diverging characteristic time scale of the process can be regarded as the origin of the weak nonergodic behavior. One might now ask what the diverging characteristic time scale for integrated Brownian motion is. For an answer to this question, one should keep in mind that pure diffusion processes (without drift) are characterized by many changes of direction, where the direction of the motion changes if the velocity changes its algebraic sign. For integrated Brownian motion, the corresponding velocity process is the Wiener process. It is well known that the mean first passage time of a Wiener trajectory to the origin starting from a certain positive or negative value does not exist. Therefore, the averaged time between changes of direction of integrated Brownian motion diverges.

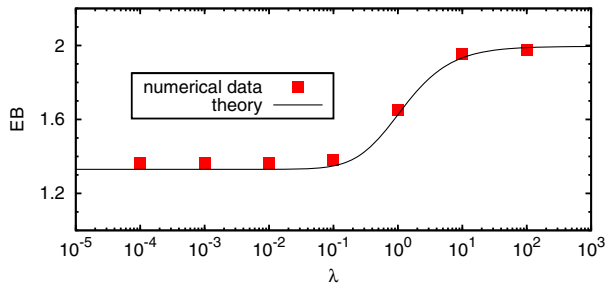

FIG. 4 (color online). Numerically obtained ergodicity breaking parameter ($\tau = 100$) for different values of $\lambda = t_a/T$ compared with EB from Eq. (12). $N = 10^5$ trajectories of length $T = 10^5$ generated by the standard map for $k = 1.5$ were used for the numerical determination.

The phase spaces of other nonlinear maps which are Poincaré sections of low-dimensional Hamiltonian systems can be locally approximated by the phase space of the standard map, where the perturbation parameter typically decreases with increasing momentum (see, e.g., Chaps. 3 and 4 in [33]). Therefore, the momentum cannot increase to arbitrarily high values but is limited by integrable structures such as invariant KAM curves. However, as long as diffusion in momentum direction is not limited by these curves, the corresponding diffusion in coordinate direction exhibits all the features of integrated Brownian motion. Furthermore, our findings are also important for higher-dimensional Hamiltonian systems, where Arnold diffusion, i.e., normal diffusion in some action variables, occurs [33]. All the phenomena discussed in this Letter apply to the corresponding angle variables, possibly with some modifications due to the resonance structures in phase space. Obviously, the results obtained in this Letter are not restricted to Hamiltonian systems, but are valid whenever normal momentum diffusion occurs. Moreover, in a future publication [57], we are going to show that integrated Brownian motion can be reduced to a special Lévy walk with a spatiotemporal coupling of the form $\psi(x,t) \propto \delta(|x| - t^{3/2})t^{-3/2}$ [63]. This stochastic process exhibits a similar type of weak nonergodicity.

We want to thank Eli Barkai for helpful discussions. Partial support from Deutsche Forschungsgemeinschaft (Grant No. RA 416/8-1) is gratefully acknowledged.

*tony.albers@physik.tu-chemnitz.de
†guenter.radons@physik.tu-chemnitz.de

[1] J.-P. Bouchaud and A. Georges, Phys. Rep. **195**, 127 (1990).
[2] R. Metzler and J. Klafter, Phys. Rep. **339**, 1 (2000).
[3] *Anomalous Transport: Foundations and Applications*, 1st ed., edited by R. Klages, G. Radons, and I. M. Sokolov, (Wiley-VCH, Weinheim, 2008).
[4] H. Scher and E. W. Montroll, Phys. Rev. B **12**, 2455 (1975).
[5] Y. Li, G. Farrher, and R. Kimmich, Phys. Rev. E **74**, 066309 (2006).
[6] I. Golding and E. C. Cox, Phys. Rev. Lett. **96**, 098102 (2006).
[7] D. Brockmann, L. Hufnagel, and T. Geisel, Nature (London) **439**, 462 (2006).
[8] C. F. F. Karney, Physica (Amsterdam) **8D**, 360 (1983).
[9] T. Geisel, A. Zacherl, and G. Radons, Phys. Rev. Lett. **59**, 2503 (1987).
[10] G. Zumofen and J. Klafter, Europhys. Lett. **25**, 565 (1994).
[11] D. del Castillo-Negrete, Phys. Fluids **10**, 576 (1998).
[12] D. del Castillo-Negrete, Phys. Plasmas **7**, 1702 (2000).
[13] The symbol $\langle D_\alpha \rangle$ for the generalized diffusion coefficient indicates that it is the first moment of the distribution of generalized diffusivities introduced in [14].
[14] T. Albers and G. Radons, Europhys. Lett. **102**, 40006 (2013).
[15] E. Barkai, Y. Garini, and R. Metzler, Phys. Today **65**, No. 8, 29 (2012).
[16] R. Metzler and J.-H. Jeon, Phys. Scr. **86**, 058510 (2012).
[17] E. W. Montroll and G. H. Weiss, J. Math. Phys. (N.Y.) **6**, 167 (1965).
[18] E. Barkai and Y.-C. Cheng, J. Chem. Phys. **118**, 6167 (2003).
[19] A. Lubelski, I. M. Sokolov, and J. Klafter, Phys. Rev. Lett. **100**, 250602 (2008).
[20] Y. He, S. Burov, R. Metzler, and E. Barkai, Phys. Rev. Lett. **101**, 058101 (2008).
[21] J. H. P. Schulz, E. Barkai, and R. Metzler, Phys. Rev. Lett. **110**, 020602 (2013).
[22] B. B. Mandelbrot and J. W. V. Ness, SIAM Rev. **10**, 422 (1968).
[23] S. Havlin and D. Ben-Avraham, Adv. Phys. **36**, 695 (1987).
[24] W. Deng and E. Barkai, Phys. Rev. E **79**, 011112 (2009).
[25] Y. Meroz, I. M. Sokolov, and J. Klafter, Phys. Rev. E **81**, 010101 (2010).
[26] J. P. Bouchaud, J. Phys. I (France) **2**, 1705 (1992).
[27] X. Brokmann, J.-P. Hermier, G. Messin, P. Desbiolles, J.-P. Bouchaud, and M. Dahan, Phys. Rev. Lett. **90**, 120601 (2003).
[28] J.-H. Jeon, V. Tejedor, S. Burov, E. Barkai, C. Selhuber-Unkel, K. Berg-Sørensen, L. Oddershede, and R. Metzler, Phys. Rev. Lett. **106**, 048103 (2011).
[29] A. G. Cherstvy, A. V. Chechkin, and R. Metzler, New J. Phys. **15**, 083039 (2013).
[30] M. F. Shlesinger, B. J. West, and J. Klafter, Phys. Rev. Lett. **58**, 1100 (1987).
[31] A. Godec and R. Metzler, Phys. Rev. Lett. **110**, 020603 (2013).
[32] D. Froemberg and E. Barkai, Phys. Rev. E **87**, 030104 (2013).
[33] A. J. Lichtenberg and M. A. Lieberman, *Regular and Chaotic Dynamics*, 2nd ed. (Springer-Verlag, New York, 1992).
[34] L. Kaplan, Phys. Rev. Lett. **89**, 184103 (2002).
[35] J. J. Metzger, R. Fleischmann, and T. Geisel, Phys. Rev. Lett. **105**, 020601 (2010).
[36] M. A. Topinka, B. J. LeRoy, R. M. Westervelt, S. E. J. Shaw, R. Fleischmann, E. J. Heller, K. D. Maranowski, and A. C. Gossard, Nature (London) **410**, 183 (2001).
[37] E. J. Heller, L. Kaplan, and A. Dahlen, J. Geophys. Res. **113**, C09023 (2008).
[38] H. Kesten and G. C. Papanicolaou, Commun. Math. Phys. **78**, 19 (1980).
[39] D. Dürr, S. Goldstein, and J. L. Lebowitz, Commun. Math. Phys. **113**, 209 (1987).
[40] B. Gadway, J. Reeves, L. Krinner, and D. Schneble, Phys. Rev. Lett. **110**, 190401 (2013).
[41] S. J. Cornell, M. R. Swift, and A. J. Bray, Phys. Rev. Lett. **81**, 1142 (1998).
[42] G. D. Smedt, C. Godrèche, and J. M. Luck, Europhys. Lett. **53**, 438 (2001).
[43] T. W. Burkhardt, J. Phys. A **26**, L1157 (1993).
[44] L. F. Richardson, Proc. R. Soc. A **110**, 709 (1926).
[45] A. M. Obukhov, Adv. Geophys. **6**, 113 (1959).
[46] D. A. Kessler and E. Barkai, Phys. Rev. Lett. **108**, 230602 (2012).
[47] J. Duplat, S. Kheifets, T. Li, M. G. Raizen, and E. Villermaux, Phys. Rev. E **87**, 020105 (2013).
[48] B. V. Chirikov, Phys. Rep. **52**, 263 (1979).
[49] J. M. Greene, J. Math. Phys. (N.Y.) **20**, 1183 (1979).
[50] A. B. Rechester and R. B. White, Phys. Rev. Lett. **44**, 1586 (1980).
[51] For $k > 2$ there are also certain ranges of the perturbation parameter, where diffusion is superdiffusive due to the appearance of accelerator modes [52].
[52] Y. H. Ichikawa, T. Kamimura, and T. Hatori, Physica (Amsterdam) **29D**, 247 (1987).
[53] R. S. MacKay, J. D. Meiss, and I. C. Percival, Phys. Rev. Lett. **52**, 697 (1984).
[54] A. Kolmogoroff, Ann. Math. **35**, 116 (1934).
[55] H. P. McKean, Jr., Journal of mathematics of Kyoto University **2**, 227 (1963).
[56] F. E. Beichelt and L. P. Fatti, *Stochastic Processes and Their Applications*, 1st ed. (CRC Press, Boca Raton, FL, 2002).
[57] T. Albers and G. Radons (to be published).
[58] R. Kubo, Rep. Prog. Phys. **29**, 255 (1966).
[59] M. Kac, Trans. Am. Math. Soc. **65**, 1 (1949).
[60] P. P. Valkó and J. Abate, Comput. Math. Appl. **48**, 629 (2004).
[61] R. H. Cameron and W. T. Martin, Bull. Am. Math. Soc. **51**, 73 (1945).
[62] S. S. Stepanov, *Stochastic World*, 1st ed. (Springer, New York, 2013).
[63] G. Zumofen, A. Blumen, J. Klafter, and M. F. Shlesinger, J. Stat. Phys. **54**, 1519 (1989).